Proceedings of the IASS Annual Symposium 2016
"Spatial Structures in the 21st Century"
26–30 September, 2016, Tokyo, Japan
K. Kawaguchi, M. Ohsaki, T. Takeuchi (eds.)

Curvature in Kirigami Sheets

S.R. WILSON*, K.A. SEFFEN

Advanced Structures Group Laboratory
Department of Engineering
Cambridge University
Trumpington Street, Cambridge CB2 1PZ, UK
*srw57@cam.ac.uk, kas14@cam.ac.uk

Abstract

Kirigami design differs from origami by allowing cuts and material removal in addition to folding. This work explores the use of kirigami as a basis for transforming flat sheets into 3D shapes. By formulating the principles of kirigami with topology and differential geometry, a framework is developed for transforming a sheet between flat and curved configurations by "suturing" cuts in a sheet. This framework is demonstrated by designing and analyzing a kirigami unit cell. We find that this unit cell is a type of plane symmetric 6R linkage. We analyze the linkage and illustrate two possible tessellations. Planar design suitable for standard subtractive machining processes ensures the manufacturability of the structures. We expect this system to find applications in morphing structures and robotics where transitions between curvature states are desired.

Keywords: Origami, Kirigami, Reconfigurable, Transformable, Tessellation, Gauss Map, Topology, Lattice, Curvature, Overconstrained Linkage

1. Introduction

Kirigami, the art of cutting paper, has recently emerged as an alternative to origami for manufacturing three-dimensional (3D) geometries from two dimensions (2D). While origami has drawbacks such as excess material and intricate folds, kirigami techniques circumvent these difficulties by removing excess material and producing objects with simple folds. Information for 3D shapes is programmed into 2D sheets through the geometry of cuts. The principles underpinning these cuts are an active topic of research, and open questions remain, such as generalized cutting rules that will allow embedding of the sheet in three dimensions [1].

This work is motivated by the increasing demand for responsive architectures— interactive objects that respond to their environment. Research in this mode has presented shape-changing surfaces for aerodynamic designs, solar panels, and robotics [2, 3]. This work explores kirigami as a modular framework for transformable surface architecture. So-called "pluripotent" materials have been explored to produce out-of-plane geometry from kirigami, where the distribution of cuts made in a sheet are limited to a hexagonal graph and its triangular dual [4]. Rules are devised and experiments approximate curvature through the use of basic geometric building blocks. The result is a height map where the achievable gradient is limited by the size of the chosen unit cell. Similar schemes have been explored on the nano-scale using graphene [5].

Morphing structure design is rooted in repeating unit cell constructions. The geometry of the unit cell is analyzed and exploited through tessellation, such as the Miura-Ori geometry [2, 6–8]. The generalized problem of foldable sheets has been solved algorithmically, analytically, and computationally [9–11]. In

robotics, the mathematical principles of folding have been applied to produce actuated structures [12–14]. In the generalized schemes, each polygonal element of the sheet is thought to be rigid or to allow bending of the first order [15].
This work rebuilds the foundations of kirigami from topological principles to its geometric implications, and results in the design and analysis of a kirigami unit cell. Links are drawn between kirigami and overconstrained linkages, and this similarity is employed to determine tessellation rules for multiple degree-of-freedom kirigami networks. We envision a reconfigurable surface composed of kirigami units that is able to change between a variety of global mode shapes. We hope for this work to elucidate the principles of morphing kirigami design and to find a variety of applications.

2. Topology

Given a finite surface, we define "holes" as the removal of material from a sheet in the form of a finite topological disc within the original sheet which does not disturb the boundary of that sheet. The Euler characteristic of a polyhedral surface is defined as [8]

$$\chi = V - E + F \tag{1}$$

where V, E and F are the number of vertices, edges, and faces respectively in the sheet. A face is said to be simply connected such that no contour within the face may surround a hole. χ is 1 for a disc while χ is 0 for an annulus (a disc with a single hole). For each additional hole, χ is decreased by 1 for the sheet, which can be proven by induction. Thus, a perforated sheet has a characteristic

$$\chi_s = \chi_d - g(\chi_d) = 1 - g \tag{2}$$

where g is the number of perforations and χ_d is 1 for a disc: this is a direct analog to closed orientable objects of genus g where g is the number of handles and χ_{toroid} is $2 - 2g$ such that χ_s is $\frac{1}{2}\chi_{toroid}$ [16]. This basic topological analysis is enlightening for the design of a kirigami surface; each original hole can be closed to alter the total curvature of the sheet by 2π, changing the object's homotopy group. By designing cuts strategically within a sheet, we are able to change the geometry of that sheet by closing these cuts. We seek a building block to create a global shape— a repeating unit to transform the sheet between homotopy groups. And by programming the state of each unit cell, we can achieve an array of global shapes.

3. Geometry

Topological principles are not concerned with physical materials resistant to large in-plane deformations. Thus, we use geometry to link the topology of a perforated sheet to its physical existence. This link is the Gauss-Bonnet Theorem [16]

$$\int_{\delta A} K \, \mathrm{d}A + \int_{\delta S} k_g \, \mathrm{d}S = 2\pi\chi \tag{3}$$

where K is the Gaussian curvature within the surface and k_g is the geodesic curvature along the surface boundaries. This equation provides a global curvature invariant of a surface based on χ from Eqn (1). For the perforated disc we can insert Eqn (2) resulting in

$$\int_{\delta A} K \, \mathrm{d}A + \int_{\delta S} k_g \, \mathrm{d}S = 2\pi(1 - g). \tag{4}$$

For discrete polyhedral surfaces bounded by n geodesics each of curvature k_g

$$\sum_{i=1}^{n} \int_{\delta S_i} k_g \, \mathrm{d}s = 0. \tag{5}$$

The geodesics in the plane are straight line segments (edges), and boundary curvature is defined by the turning angles of the edges. The Gauss-Bonnet Theorem for a polyhedral surfaces composed of planar facets can then be rewritten using Descartes' Theorem for the turning angles as

$$\int_{\delta A} K \, \mathrm{d}A + \sum_{i=1}^{n} \pi - \alpha_i = 2\pi(1 - g) \tag{6}$$

where α_i is the interior angle of a polygonal facet. It can be shown that the Gaussian curvature concentrated at a polyhedral vertex v is exactly d, the angle defect of that vertex [17]. Since we restrict all facets to be rigid and planar, the integral of the Gaussian curvature over the surface is equal to the sum of the interior angle defects and each vertex defect is equal to the solid angle subtended by a Gauss map of that vertex with area

$$A = (2 - n)\pi + \sum_{i=1}^{n} \beta_i \tag{7}$$

where β_i is the interior angle of the i^{th} facet of the surface meeting at vertex v with n facets. It is trivial to show that α_i is equivalent to $\pi - \beta_i$ and the angle defect of a polyhedral vertex is defined as

$$d(v) = 2\pi - \sum_{i=1}^{n} \alpha_i. \tag{8}$$

Combining Eqn (6) and Section 3, the Gauss-Bonnet theorem is rewritten as

$$2\pi - \sum_{i=1}^{n} \alpha_i + \sum_{i=1}^{n} \pi - \alpha_i = 2\pi(1 - g) \tag{9}$$

for a discrete polyhedral surface with planar facets. This analysis is employed in computational geometry as a straightforward method of calculating a discrete curvature for a polyhedral mesh [18]. We wish to use this framework to explore the curvature of our kirigami unit cell. By constructing a series of Gauss maps, it becomes clear how the curvature of the surface changes throughout its transformation.

4. Unit Cell

Cutting a disc from a thin sheet and joining the edges of the hole together produces a minimal surface containing a saddle and two peaks [19]. Discretizing the disc into a rhombus results in the simplest hole that can be completely closed along straight edges. This is a form of the square lattice kirigami shown in Fig. 1. With the removal of two fold lines, we obtain a single degree of freedom mechanism containing a rhomboidal hole, as shown in Fig. 2. We first apply the discrete Gauss-Bonnet theorem to the vertices of the unit cell in the open configuration and the closed configuration. As the topology is fixed, we analyze the geometry of the cell using the vector parameterization shown in Fig. 2.
In the open configuration, summing the interior angles and the exterior turning angles of Fig. 3 yields

$$[2(2\alpha) + 2(\pi - 2\alpha)] + [4(\pi - \alpha_{ext,2} + 2(\pi - \alpha_{ext,1})] = 2\pi\chi = 0 \tag{10}$$

where the exterior angles are:

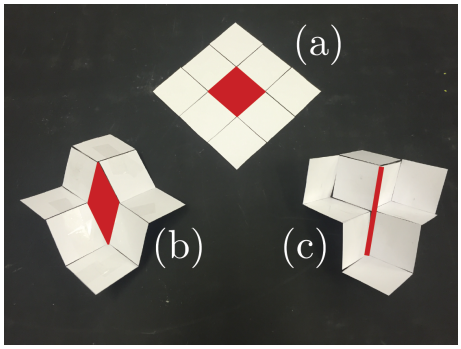

Figure 1: Basic square lattice kirigami. (a) Flat, unfolded annulus state. (b) Transition state. (c) Sutured disc state with hole fully closed.

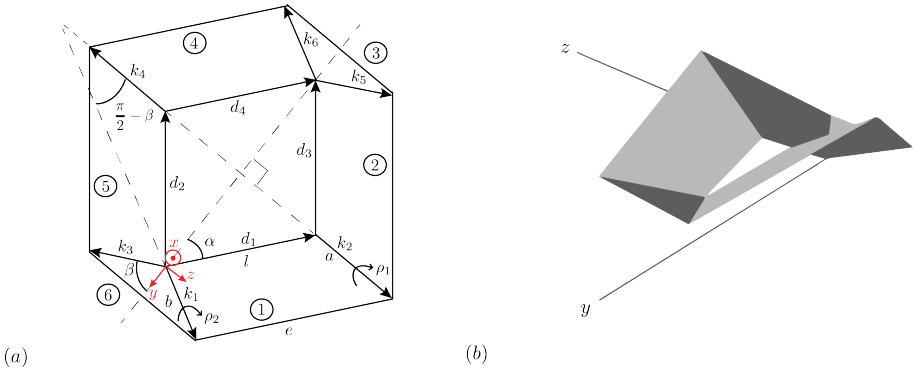

Figure 2: (a) Geometric parameterization of a one degree-of-freedom kirigami unit cell in its planar state. Vectors labeled *k* are fold lines; those labeled *d* are hole edges. (b) Rendering of the unit cell in a partially folded configuration. The origin (of the coordinates shown in red) is placed in the same position as in the parametric analysis.

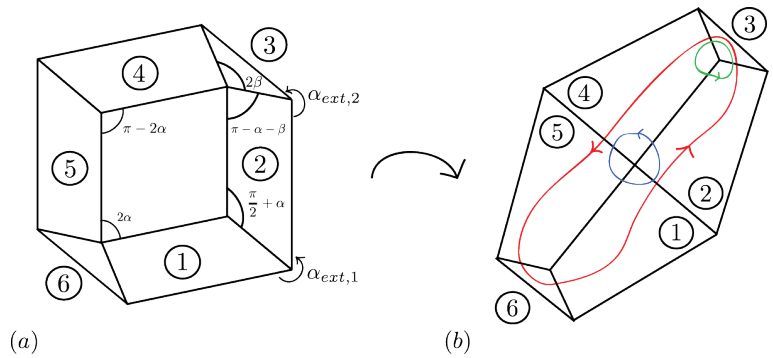

Figure 3: Two extreme states of the unit cell from Fig. 2. (a) The open planar state shows the unique interior and exterior vertex angles. (b) The closed configuration in plan view shows the contours used to produce Gauss maps. The green and blue contours yield the positive and negative Gauss maps for individual vertices, respectively, while the red contour yields the gauss map of the interior of the unit cell in its closed configuration. These maps are shown in Figs 4 and 5, respectively.

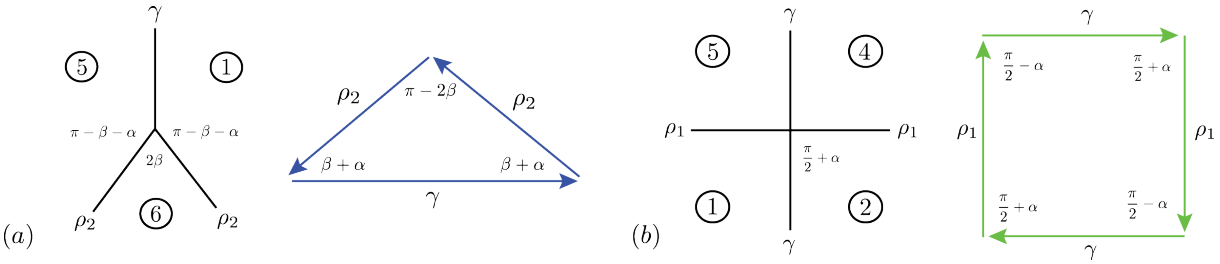

Figure 4: (a) One of two angular defect vertices in the interior of the closed until cell and its corresponding Gauss map. (b) The center saddle vertex of the closed unit cell and its corresponding Gauss map.

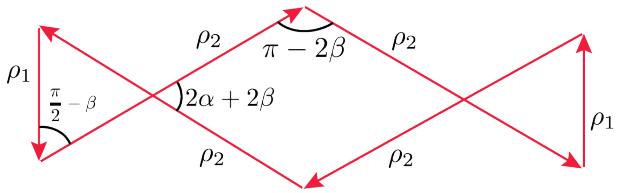

Figure 5: Gauss map of the three interior vertices in the closed configuration of the unit cell. The total solid angle as a sum of each signed area is zero; thus, the interior holds no net Gaussian curvature as expected.

$$\alpha_{ext,1} = \pi + 2\alpha, \qquad \alpha_{ext,2} = \frac{3\pi}{2} - \alpha \tag{11}$$

and χ is 0 for an annulus; in the closed configuration χ is 1. The angular defect computation becomes a calculation of spherical polygon area, denoted A_{quad} and A_{tri} for the area of a spherical quadrilateral and triangle, respectively:

$$A_{quad} = \sum_{i}^{3} \alpha_i - 2\pi = 2(\pi - 2\beta) + 2(2\alpha + 2\beta) - 2\pi = 4\alpha \tag{12}$$

$$A_{tri} = \sum_{i}^{3} \alpha_i - \pi = 2(\frac{\pi}{2} - \beta) + (2\alpha + 2\alpha) = 2\alpha. \tag{13}$$

Thus, the angular defect

$$d(v) = 2(2\alpha) - 4\alpha = 0 \tag{14}$$

where the center solid angle is negative due to its clockwise direction shown in Fig. 3. We see that the curvature, upon closing a cell, shifts to the exterior vertices and sums to 2π. By tessellating unit cells, we can take advantage of this curvature shift to construct a modular sheet with global shape by the combination of changing geometries.

5. 6R Linkage

We identify an analogous linkage of the unit cell which is a special case of the 6R Bricard linkage [20], drawn in Fig. 6. A linkage with n bodies connected by g joints where joint i allows f_i freedoms is said to have a difference between mobility m and states of self-stress s according to the generalized Kutzbach criterion [21]

$$m - s = 6(n-1) - 6g + \sum_{i=1}^{g} f_i. \tag{15}$$

The unit cell is deemed to have equal mobility and states of self-stress with six bodies connected by six single degree of freedom joints. By inspection, the linkage has zero states of self stress and must have zero mobility according to the generalized Kutzbach. However, the linkage has multiple mobility modes due to geometric symmetry. This overconstrained linkage is ideal for the purpose of a multiple degree of freedom sheet because it allows a single actuator to change the shape of a cell while influencing the global structure. To analyze the kinematics, we use a modified form of the Denavit-Hartenberg parameters [22]. Because all hinges lie in the plane for a kirigami sheet, we do not require homogenous coordinates to compute offset axes. All adjacent fold axes meet at a point, requiring just rotations around two axes, as shown in Fig. 6. Thus, each composite transformation is a 3x3 orthogonal matrix

$$T_{ij} = \begin{bmatrix} \cos\theta_{\mathrm{i}} & -\sin\theta_{\mathrm{i}} & 0 \\ \cos\alpha_{\mathrm{i}}\sin\theta_{\mathrm{i}} & \cos\theta_{\mathrm{i}}\cos\alpha_{\mathrm{i}} & -\sin\alpha_{\mathrm{i}} \\ \sin\alpha_{\mathrm{i}}\sin\theta_{\mathrm{i}} & \cos\theta_{\mathrm{i}}\sin\alpha_{\mathrm{i}} & \cos\alpha_{\mathrm{i}} \end{bmatrix} \tag{16}$$

where T_{ij} is the transformation from link i to link j shown in Fig. 6. Using symmetry, we set two opposing composite transformations equal to find a closure condition for the linkage

$$[T_{12}][T_{23}][T_{34}] = [T_{61}]^T[T_{56}]^T[T_{45}]^T \tag{17}$$

where the sector angles α and fold angles θ about the x and z axes shown in Fig. 6 adhere to the following relationships

$$\begin{aligned} \alpha_1 = \alpha_2 = \alpha_4 = \alpha_5 = \frac{\pi}{2} - \beta;\ \alpha_3 = \alpha_4 = 2\beta \\ \theta_1 = \theta_3 = \theta_4 = \theta_6 = \rho_2;\ \theta_2 = \theta_5 = \rho_1. \end{aligned} \tag{18}$$

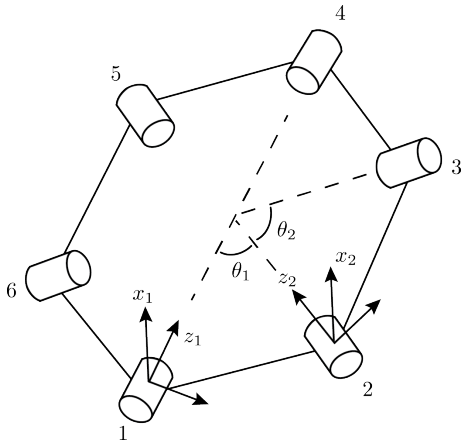

Figure 6: The 6R linkage analog to the kirigami unit cell, shown in its inital planar configuration. Coordinate transformations are made from joint 1 to joint 4 in both directions around the loop to generate a closure condition based on a modified Denavit-Hartenburg protocol.

By analyzing the closure condition in Eqn (17), we identify a periodic isosurface which visualizes the continuous motions of the linkage as a function of β, the geometric hinge angle, governed by

$$\begin{aligned}&\sin\rho_1\sin\rho_2+\sin^3\beta+\cos 2\beta\sin\beta\cos\rho_2+\sin^3\beta\cos\rho_1\cos^2\rho_2\\&+\cos 2\beta\sin\beta\cos\rho_1\cos\rho_2-\cos^2\beta\sin\beta\cos\rho_1-\sin\beta\cos\rho_1\sin\rho_2^2\\&-2\cos^2\beta\sin\rho_1\sin\rho_2-\cos^2\beta\sin\beta\cos^2\rho_2-2\sin^2\beta\cos\rho_2\sin\rho_1\sin\rho_2=0.\end{aligned}\tag{19}$$

The isosurface informs the configuration of each individual unit cell by providing an input-output relationship. Given a geometric angle β and one hinge angle, we can solve for the third unknown hinge angle which completely describes the state of the cell at any given geometry and configuration. This will inform a network of cells by providing the ability to describe the configuration of any cell within a tessellation. We plot this isosurface and numerically find the value for β for the minimum area closure loop, shown in Fig. 7. If we assume the flexural hinges in the kirigami cell to act as linear-elastic beams for a first approximation, strain energy scales linearly with hinge width. Thus, the minimum area kinematic loop is thought to correspond to the least energy geometry, the geometric design with the least amount of motion to achieve continuous transformation of the linkage.

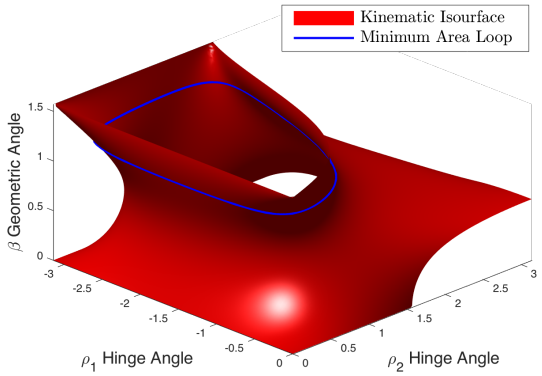

Figure 7: The isosurface is shown in red, which provides all continuous solutions given a geometric quantity β for the linkage as a function of ρ_1 and ρ_2 shown in Fig. 2. The minimum area solution for β is found and plotted as a contour in blue.

6. Tessellation

We describe a preliminary tessellation structure of the unit cell in one and two dimensions. The one dimensional network of cells is shown in various configurations in Fig. 8. By actuating n cells independently, we have 2^n possible configurations in one dimension. For a surface that is able to morph into a plethora of shapes, we seek a method of linking 1D strands together. In Fig. 9, we offer one method of tessellating in two dimensions that involves snubbing the hexagonal units into octagons and rotating the fold lines of the original unit by $\frac{\pi}{2}$. This tessellation shows promise in creating a sheet with n degrees of freedom from n unit cells. However, this pattern creates a pattern of rectangular cuts that affect the shear strength of the sheet. This may be mitigated by altering the geometry of the unit cells, and is being explored.

The current geometric and linkage analysis informs only the unit cell kinematics and geometry. In order to design a network of kirigami linkages, we must take a combinatorial approach to the problem to efficiently generate a list of geometrically plausible networks. It is nontrivial to extend a 1D tessellation into 2D due to self intersection and non-developability constraints. We can then experiment with tessellations to understand their transformations by combining the constituent unit cell kinematics. In order to devise a set of feasible tessellations, we are currently exploring methods of abstracting unit cell connections in order to systematically formulate the problem. This combinatorial formulation remains our principle challenge.

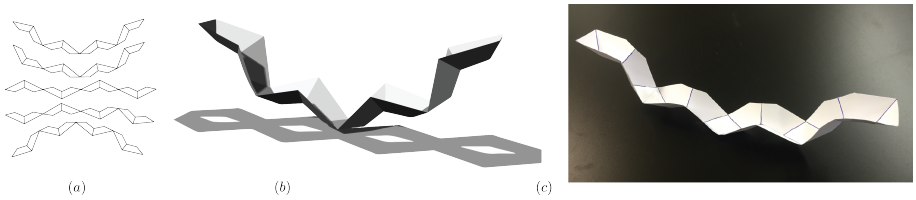

Figure 8: (a) For a one dimensional tessellation with n units, we have 2^n configurations, with five shown. By adjusting the geometry of the unit, we can create tessellations in a range of shapes. (b) Rendering of one configuration. (c) Physical prototype.

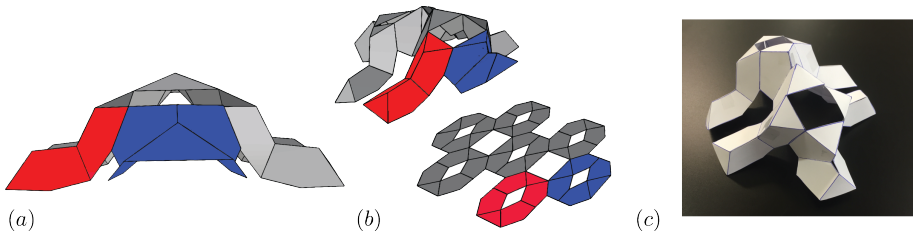

Figure 9: A possible tessellation in two dimensions. All units are closed in the same sense here, approximating a doubly curved sheet. The tessellation uses two unique unit cells shown in red and blue, with hinge lines rotated by $\frac{\pi}{2}$. (a) Side view of the tessellation. (b) Isometric view with the unfolded configuration. (c) Physical model.

7. Conclusion

We present preliminary work towards a new approach for kirigami engineering utilizing unit cell construction. Using basic differential geometry, we illustrate how a shift in curvature for a polyhedral unit cell occurs when changing homotopy groups. We outline a framework for creating surfaces exploiting this curvature shift that are able to morph in a general manner using modular units. By creating a network of n continuously kinematic linkages, we propose an n-degree of freedom surface for unit-by-unit, distributed actuation to produce an array of shapes. By characterizing the motion of the unit cell, we can combine cells to describe the shape of the actuated network.
This method of shape change is likened to muscle architecture, and could show promise in the generation of undulatory motion. Using a regular pattern of kirigami cuts with irregular closure patterns over the sheet, this scheme is the foundation for a distributed actuation of a patterned sheet in order to produce a variety of shapes. The authors are working to build a working prototype to physically realize the design and identify new problems.

Acknowledgments

The authors thank the Marshall Scholarship for supporting SRW, Prof. SD Guest for stimulating discussions on symmetry and mobility, and Tim Watson for helpful conversations on mathematical and digital modeling.

References

[1] Toen Castle, Yigil Cho, Xingting Gong, Euiyeon Jung, Daniel M. Sussman, Shu Yang, and Randall D. Kamien. Making the cut: lattice kirigami rules. *Phys. Rev. Lett.*, 113(24):1–5, 2014.

[2] J. L. Silverberg, a. a. Evans, L. McLeod, R. C. Hayward, T. Hull, C. D. Santangelo, and I. Cohen. Using origami design principles to fold reprogrammable mechanical metamaterials. *Science (80-.).*, 345(6197):647–650, 2014.

[3] Jongmin Shim, Claude Perdigou, Elizabeth R. Chen, Katia Bertoldi, and Pedro M. Reis. Buckling-induced encapsulation of structured elastic shells under pressure. *Proc. Natl. Acad. Sci.*, 109(16):5978–5983, 2012.

[4] Daniel M. Sussman, Yigil Cho, Toen Castle, Xingting Gong, Euiyeon Jung, Shu Yang, and Randall D. Kamien. Algorithmic lattice kirigami: A route to pluripotent materials. *Proc. Natl. Acad. Sci. U. S. A.*, 112(24):7449–7453, 2015.

[5] Melina K. Blees, Arthur W. Barnard, Peter a. Rose, Samantha P. Roberts, Kathryn L. McGill, Pinshane Y. Huang, Alexander R. Ruyack, Joshua W. Kevek, Bryce Kobrin, David a. Muller, and Paul L. McEuen. Graphene kirigami. *Nature*, 2015.

[6] Mark Schenk and Simon D. Guest. Geometry of Miura-folded metamaterials. *Proc. Natl. Acad. Sci.*, 110(9):3276–3281, 2013.

[7] Kenneth C Cheung, Tomohiro Tachi, Sam Calisch, and Koryo Miura. Origami interleaved tube cellular materials. *Smart Mater. Struct.*, 23(9):094012, 2014.

[8] Bryan Gin-ge Chen, Bin Liu, Arthur A. Evans, Jayson Paulose, Itai Cohen, Vincenzo Vitelli, and C. D. Santangelo. Topological mechanics of origami and kirigami. *arXiv Prepr. arXiv1508.00795*, 2:1–11, 2015.

[9] Erik D. Demaine and Joseph O'Rourke. *Geometric Folding Algorithms: Linkages, Origami, Polyhedra*. Cambridge University Press, 2007.

[10] Wolfgang K Schief, Alexander I Bobenko, and Tim Hoffmann. On the integrability of infinitesimal and finite deformations of polyhedral surfaces. In *Discret. Differ. Geom.*, volume 38, pages 67–93. Birkhauser Basel, 2008.

[11] Tomohiro Tachi. Generalization of rigid foldable quadrilateral mesh origami. *J. Int. Assoc. Shell Spat. Struct.*, 50(October):2287–2294, 2009.

[12] Cagdas D Onal, Robert J Wood, and Daniela Rus. Towards Printable Robotics : Origami-inspired planar fabrication of three-dimensional mechanisms. In *IEEE Int. Conf. Robot. Autom.*, pages 4608–4613, Shanghai, 2011. IEEE.

[13] E Hawkes, B An, N M Benbernou, H Tanaka, S Kim, E D Demaine, D Rus, and R J Wood. Programmable matter by folding. *Proc. Natl. Acad. Sci. U. S. A.*, 107(28):12441–5, 2010.

[14] Kyle Gilpin and Daniela Rus. Modular robot systems from self-assembly to self- disassembly. *IEEE Robot. Autom. Mag.*, pages 38–55, 2010.

[15] Mark Schenk and Simon D. Guest. Folded textured sheets. In *Proc. Int. Assoc. Shell Spat. Struct. Symp.*, number October, pages 2328–2336, 2010.

[16] Oliver Knill. A discrete Gauss-Bonnet type theorem. *Elem. der Math.*, 67:1–17, 2012.

[17] C. R. Calladine and J. L. Sanders. *Theory of Shell Structures*, volume 51. Cambridge University Press, 1984.

[18] Lyuba Alboul, Gilberto Echeverria, and Marcos Rodrigues. Discrete curvatures and Gauss maps for polyhedral surfaces. *Eur. Work. Comput. Geom.*, pages 9–12, 2005.

[19] Jemal Guven, J. A. Hanna, Osman Kahraman, and Martin Michael Müller. Dipoles in thin sheets. *Eur. Phys. J. E*, 36(9):18, 2013.

[20] Yan Chen, Zhong You, and Tibor Tarnai. Threefold-symmetric Bricard linkages for deployable structures. *Int. J. Solids Struct.*, 42(8):2287–2301, 2005.

[21] S. D. Guest and P. W. Fowler. A symmetry-extended mobility rule. *Mech. Mach. Theory*, 40(9):1002–1014, 2005.

[22] Sarah-Marie Belcastro and Thomas C. Hull. Modelling the folding of paper into three dimensions using affine transformations. *Linear Algebra Appl.*, 348(1-3):273–282, 2002.